Electronic Supplementary Information

A Self-Assembly Toolbox for Thiophene-Based Conjugated Polyelectrolytes: Surfactants, Solvent and Copolymerisation

Judith E. Houston,*[a] Michèle Chevrier,[b] Marie-Sousai Appavou,[a] Stephen M. King,[c] Sébastien Clément*[b] and Rachel C. Evans*[d]

[a] *Jülich Centre for Neutron Science (JCNS) at Heinz Maier-Leibnitz Zentrum (MLZ), Forschungszentrum Jülich GmbH, Lichtenbergstr. 1, 85748 Garching, Germany. Email: j.houston@fz-juelich.de*
[b] *Institut Charles Gerhardt – UMR 5253, Université de Montpellier – CC1701, Place Eugène Bataillon, F-34095 Montpellier Cedex 05, France. Email: sebastien.clement1@umontpellier.fr*
[c] *ISIS Facility, STFC Rutherford Appleton Laboratory, Harwell Campus, Didcot, Oxon, OX11 0QX, United Kingdom.*
[d] *Department of Materials Science & Metallurgy, University of Cambridge, 27 Charles Babbage Road, Cambridge, CB3 0FS, United Kingdom. Email: rce26@cam.ac.uk*

Table of Contents

1. Sample Compositions

Table S1. Composition of **P3HTPMe$_3$(SDS)$_x$** samples.

x	P3HTPMe$_3$ conc. (mg mL^{-1})	SDS conc. (mg mL^{-1})
0.2	8.48	1.52
0.5	6.91	3.09
1.0	5.27	4.73
2.0	3.58	6.42
5.0	1.82	8.18
20.0	0.53	9.47

Table S2. Composition of **P3HT-*b*-P3HTPMe$_3$(SDS)$_x$** samples.

x	P3HT-*b*-P3HTPMe$_3$ conc. (mg mL^{-1})	SDS conc. (mg mL^{-1})
0.2	9.12	0.88
0.5	8.06	1.94
1.0	6.75	3.25
2.0	5.09	4.91
5.0	2.94	7.06
20.0	0.94	9.06

2. Optical Studies on P3HTPMe$_3$- and P3HT-*b*-P3HTPMe$_3$-Surfactant Complexes

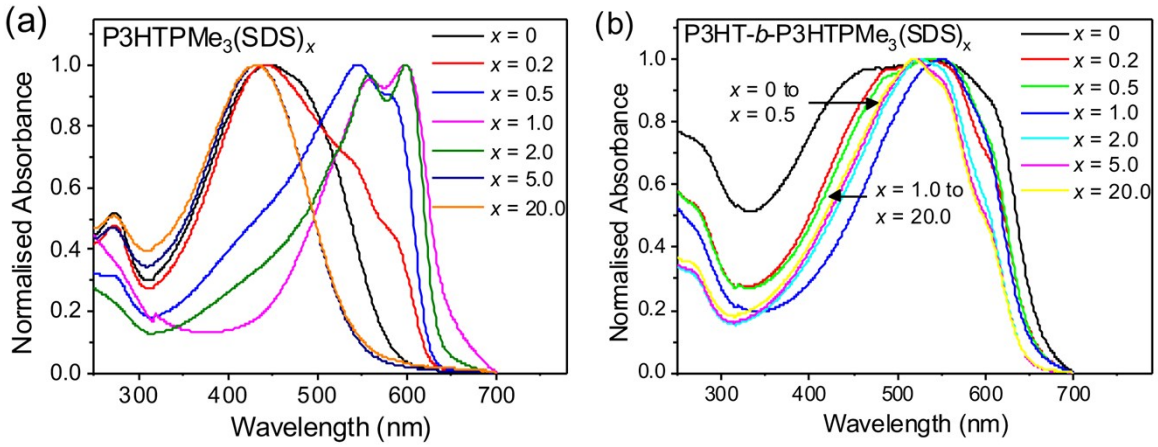

Figure S1. Normalised UV/Vis absorption spectra for (a) **P3HTPMe$_3$(SDS)$_x$** and (b) **P3HT-*b*-P3HTPMe$_3$(SDS)$_x$** as a function of composition, *x*, at room temperature. Total sample concentration = 0.1 mg mL^{-1} in D_2O.

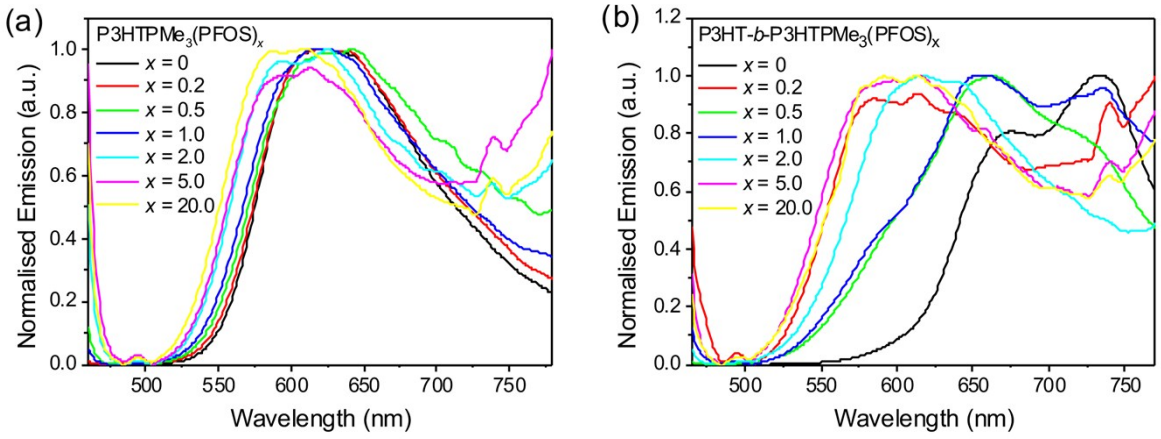

Figure S2. Normalised steady-state emission spectra for (a) **P3HTPMe$_3$(PFOS)**$_x$ and (b) **P3HT-*b*-P3HTPMe$_3$(PFOS)**$_x$ as a function of PFOS composition, x, at room temperature. Total sample concentration = 10 mg mL^{-1} in D_2O. λ_{ex} = 450 nm.

3. SANS Data Analysis of CPE-Surfactant Complexes

3.1 SANS Form Factor Models

The SANS scattering profiles were modelled using a non-linear least squares method in the SasView programme version 3.1.2 on a Windows 10 64-bit operating system.[1] The scattered SANS intensity for the following aggregate shapes is given by:

$$I(q) = NV^2P(q)S(q) + B_{inc} \quad \text{(S1)}$$

where N is the number of particles per unit volume, V is the volume of the aggregate, $P(q)$ is the form or shape factor, $S(q)$ is the structure factor and B_{inc} is the isotropic incoherent background signal. Figure S3 shows a pictorial representation of the form factor models discussed in the article. Unless otherwise stated the data were fit over the entire q-range of 0.08 < q < 2.2 nm^{-1}.

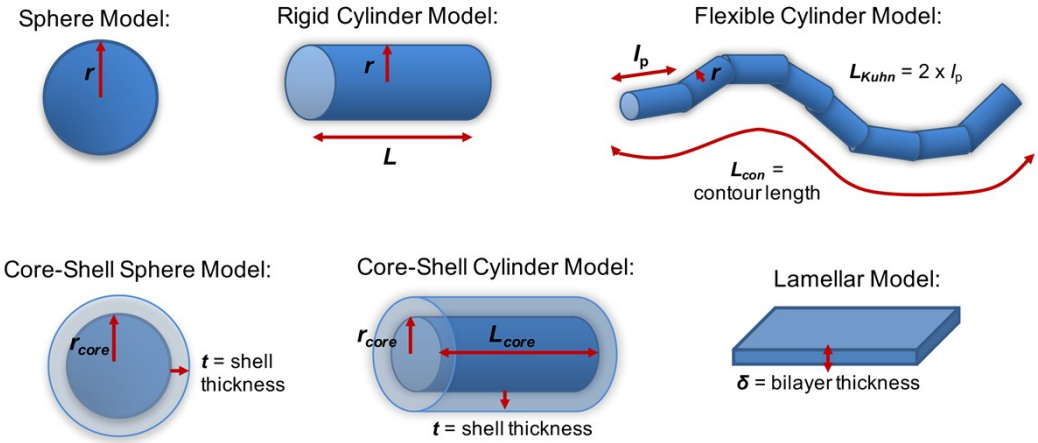

Figure S3. Schematic illustrations of the form factors, $P(q)$, used in the SANS fitting procedure. r is the radius of a sphere or cylinder, L is the length of a cylinder, l_p is the persistence length, L_{Kuhn} is the Kuhn length, and r_{core} and L_{core} are the radius and length of a core, respectively.

3.1.1 Spherical Model

This model provides the form factor, $P(q)$, for monodisperse spherical particles with uniform scattering length density. The form factor is normalised by the particle volume, V.[2]

$$P(q) = \frac{scale}{V}\left[\frac{3V(\Delta\rho)(\sin(qr) - qr\cos(qr))}{(qr)^3}\right]^2 + B_{inc} \quad \text{(S2)}$$

where *scale* is a volume fraction, r is the radius of the sphere, $\Delta\rho$ (contrast) is the difference in scattering length density (SLD) between the scatterer (sphere) and the solvent and B_{inc} is the isotropic incoherent background signal.

3.1.2 Rigid Cylinder Model

The form or shape factor, $P(q, \alpha)$, for the Cylinder model is given by:[2, 3]

$$P(q,\alpha) = \frac{scale}{V}\int_0^{\pi/2} f^2(q)\sin\alpha d\alpha + B_{inc} \quad \text{(S3)}$$

where

$$f(q) = 2V(\Delta\rho)\frac{J_1(qr\sin\alpha)}{qr\sin\alpha}\frac{sin(\frac{qL\cos\alpha}{2})}{\frac{qL\cos\alpha}{2}} \quad \text{(S4)}$$

where α is the angle between the axis of the cylinder and the q-vector, V is the total volume of the cylinder, L is the cylinder length, r is the radius of the cylinder, $\Delta\rho$ (contrast) is the difference in SLD between the scatterer (cylinder) and the solvent. J_1 is the first order Bessel function of the first kind. The form factor is normalised by the particle volume so that the scale factor of the fit is the total particle volume fraction $\varphi = NV_s$ when $I(q)$ has been correctly reduced to absolute units.

3.1.3 Core-Shell-Sphere Model

The form factor, $P(q)$, for the Core-Shell-Sphere model is given by:[2]

$$\varphi V_s P(q) = \frac{scale}{V_s} f^2(q) \quad \text{(S5)}$$

where

$$f(q) = 3V_c(\rho_c - \rho_s)\frac{\left[\sin(qr_c) - qr_c\cos(qr_c)\right]}{(qr_c)^3} + 3V_S(\rho_c - \rho_{solv})\frac{\left[\sin(qr_s) - qr_c\cos(qr_s)\right]}{(qr_s)^3} \quad \text{(S6)}$$

where V_s is the total volume of the outer shell, V_c is the volume of the core, r_c is the radius of the core, r_s is the radius of the core and shell, $r_s = r_c + t$ where t is the thickness of the shell, and ρ_c, ρ_s and ρ_{solv}

are the scattering length densities of the core, shell and solvent, respectively.[2] This model provides the form factor for a sphere with a core-shell SLD profile. The form factor is normalised by the particle volume so that the scale factor of the fit is the total particle volume fraction $\varphi = NV_s$ when $I(q)$ has been correctly reduced to absolute units. The fitting procedure included polydispersity in the radius of the spheres and instrumental q-smearing was applied to provide better fits at the high q end of the SANS data.

3.1.4 Core-Shell-Cylinder Model

The form or shape factor, $P(q, \alpha)$, for the Core-Shell-Cylinder model is given by:[4]

$$\varphi VsP(q,\alpha) = \frac{scale}{V_s}\int_0^{\pi/2} f^2(q)\, d\alpha \tag{S7}$$

where

$$f(q) = \frac{2(\rho_c - \rho_s)V_c \sin\left[qLcos(\frac{\alpha}{2})\right]}{\left[qLcos\left(\frac{\alpha}{2}\right)\right]}\frac{J_1[qrsin\alpha]}{[qrsin\alpha]} + \frac{2(\rho_s - \rho_{solv})V_s \sin\left[q(L+t)cos(\frac{\alpha}{2})\right]}{\left[q(L+t)cos\left(\frac{\alpha}{2}\right)\right]}\frac{J_1[q(r+t)sin\alpha]}{[q(r+t)sin\alpha]} \tag{S8}$$

where α is the angle between the axis of the cylinder and the q-vector, V_s is the total volume of the core plus shell, V_c is the volume of the core, L is the length of the core, r is the radius of the core, t is the thickness of the shell, and ρ_c, ρ_s and ρ_{solv} are the SLDs of the core, shell and solvent, respectively.[4] J_1 is the first order Bessel function of the first kind. This model provides the form factor for a cylinder with a core-shell scattering length density profile. The form factor is normalised by the particle volume.

3.1.5 Lamellar Sheet Model

The scattered SANS intensity in the lamellar model is given by:[5, 6]

$$I(q) = [2\pi VP(q)S(q)]/(dq^2) + B_{inc} \tag{S9}$$

where V is the scattering volume, d is the lamellar spacing and B_{inc} is the isotropic incoherent background signal. The interparticle structure factor, $S(q)$, which accounts for the interference of scattering from different particles in concentrated suspensions, is assumed to be one. The form factor, $P(q)$, for neutron scattering from lamellar sheets is given by:[5, 6]

$$P(q) = \frac{2\Delta\rho^2}{q^2}\left(1 - \cos(q\delta)e^{-\frac{q^2\sigma^2}{2}}\right) \tag{S10}$$

where $\Delta\rho^2$ is the difference in SLD between the scatterer and the solvent (*i.e.* the contrast), δ is the bilayer thickness and σ is arbitrarily fixed at $\delta/4$.

3.2 Procedure to Check SANS Model Fits

When possible each fit to the SANS data has been checked by calculating the theoretical volume mass of dry material the fit represents, φ_{dry}. φ_{dry} can be estimated from:

$$\varphi_{dry} = C_w \cdot \frac{P_m}{P_s} \tag{S11}$$

where C_w is the mass of solid sample in the solution, P_m is the density of the mixture of sample and solvent and P_s is the density of the solid.

3.3 Aggregation numbers

From the SANS fitting it is possible to calculate the number of polymers or surfactant molecules in an average particle using:

$$N_{agg} = \frac{V_{dry-aggregate}}{V_{molar}} \times N_A \tag{S12}$$

where N_{agg} is the aggregation number, $V_{dry\text{-}aggregate}$ is the volume of the dry aggregate, V_{molar} is the molar volume and N_A is Avogadro's number, $N_A = 6.0221 \times 10^{23}$ mol^{-1}. Note that in the case of core-shell models; $V_{dry\text{-}aggregate} = V_{dry\text{-}core} + V_{dry\text{-}shell,}$ where $V_{dry\text{-}core}$ is the volume of the dry core and $V_{dry\text{-}shell}$ is the volume of the dry shell.

3.4 Supporting SANS Figures

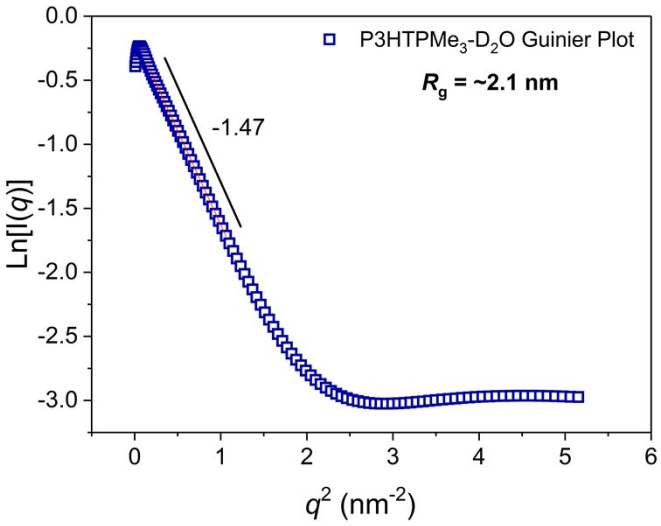

Figure S4. Guinier plot of **P3HTPMe$_3$** in D_2O (10 mg mL^{-1}) at T = 25 °C. The Guinier plot involves plotting Ln[I(q)] *vs*. q^2. The slope = $R_g^2/3$, where R_g is the radius of gyration of the scattering objects.

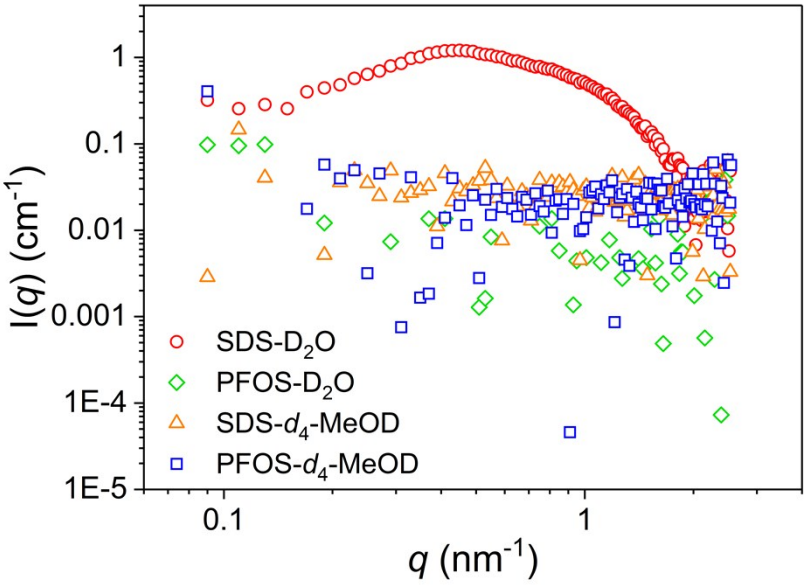

Figure S5. SANS data of SDS and PFOS in D_2O and d_4-MeOD. The concentration of each sample was 10 mg mL^{-1}. T = 25 °C. There is no clear scattering pattern observed from the surfactants in methanol, suggesting that the cmcs in MeOH are greater than the highest concentrations used in this study.

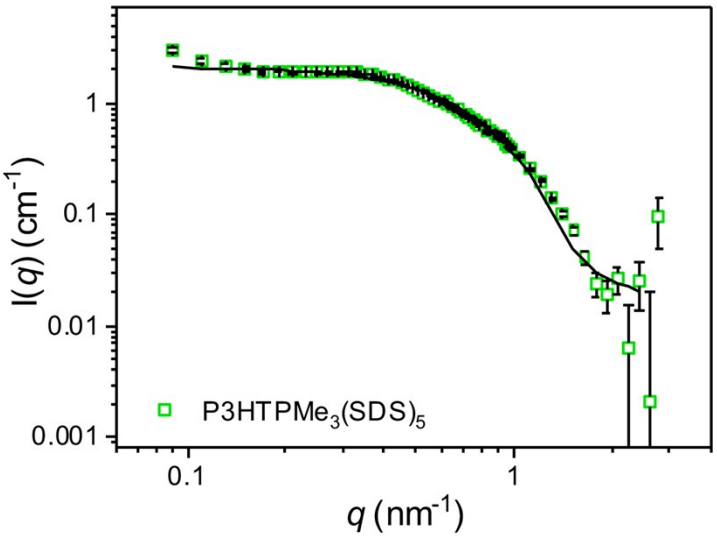

Figure S6. SANS data of **P3HTPMe$_3$(SDS)$_5$** in D_2O. The overall concentration was 10 mg mL^{-1}. T = 25 °C.

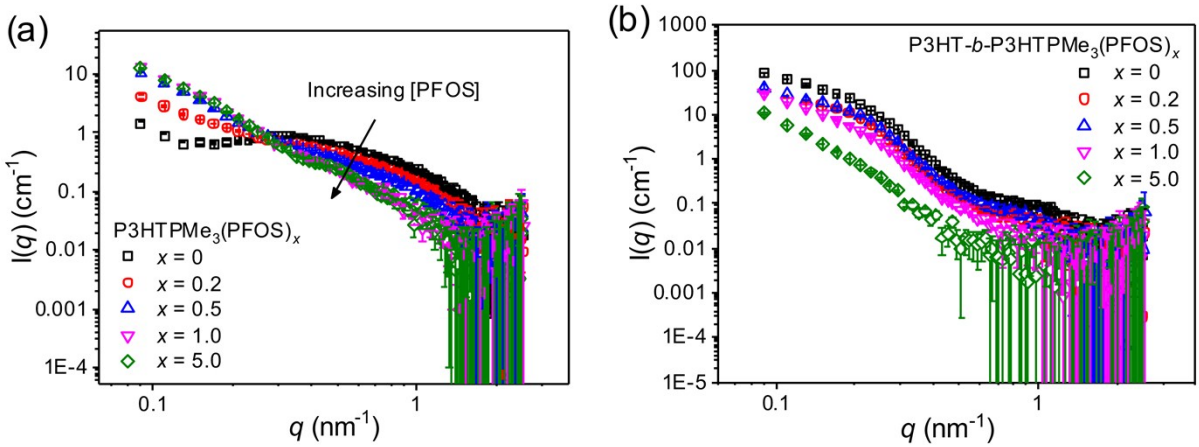

Figure S7. SANS data of (a) **P3HTPMe$_3$** and (b) **P3HT-*b*-P3HTPMe$_3$** with selected charge ratios of PFOS in D_2O. The overall concentration was 10 mg mL^{-1}. T = 25 °C.

3.5 Tables of Parameters Obtained from SANS Model Fits

3.5.1 Effect of the Surfactant (SDS) Charge Fraction on the SANS Fitting Parameters of CPE-SDS Complexes.

Table S3. Structural parameters obtained from SANS data for **P3HTPMe$_3$(SDS)$_x$** in D_2O: α is the scattering exponent of the defined q region. R_g is the radius of gyration calculated from the corresponding Guinier plot. T_{sheet} is the sheet thickness, r is the radius of the sphere or cylinder and L is the length of the cylinder obtained from the best fit to the data using the Cylinder, Lamellar and Spherical Models in SasView. X_{sol} is the calculated solvent fraction in the aggregates. Unless otherwise stated the data were fit over the entire q-range of $0.08 < q < 2.2$ nm^{-1}.

Sample	$q^{-\alpha}$ (q<0.02)	Model	R_g (nm)	r (nm)	L (nm)	T_{sheet} (nm)	X_{sol}
P3HTPMe$_3$	-	-	2.1	-	-	-	-
***x* = 0.2**	-1.71 ± 0.05	Rods	-	1.8	48.3	-	0.53
***x* = 0.5**	-2.22 ± 0.05	Sheets	-	-	-	~1.0	-
***x* = 1.0**	-2.61 ± 0.04	Sheets	-	-	-	1.8	-
***x* = 2.0**	-1.83 ± 0.01	Sheets	-	-	-	1.3	-
***x* = 5.0**	-0.46 ± 0.09	Spheres	-	2.5	-	-	0.34
***x* = 20.0**	-0.26 ± 0.10	-	1.9	-	-	-	-

Table S4. Structural parameters obtained from SANS data for **P3HTPMe$_3$(d_{25}-SDS)$_x$** in D_2O: α is the scattering exponent of the defined q region. R_g is the radius of gyration calculated from the corresponding Guinier plot. T_{sheet} is the sheet thickness, r is the radius of the sphere or cylinder and L is the length of the cylinder obtained from the best fit to the data using the Cylinder, Lamellar and Spherical Models in SasView. X_{sol} is the calculated solvent fraction in the aggregates. Unless otherwise stated the data were fit over the entire q-range of $0.08 < q < 2.2$ nm^{-1}.

Sample	$q^{-\alpha}$ **($q < 0.02$)**	**Model**	R_g **(nm)**	r **(nm)**	L **(nm)**	T_{sheet} **(nm)**
P3HTPMe$_3$	-	-	2.1	-	-	-
***x* = 0.2**	-1.30 ± 0.11	Cylinder	-	1.7	10.6	-
***x* = 0.5**	-1.97 ± 0.06	Lamellar	-	-	-	-
***x* = 1.0**	-2.69 ± 0.02	Lamellar	-	-	-	3.4
***x* = 2.0**	-1.96 ± 0.03	Lamellar	-	-	-	3.7
***x* = 5.0**	-2.08 ± 0.12	Lamellar	-	-	-	2.6
***x* = 20.0**	No scatter	-	-	-	-	-

Table S5. Structural parameters obtained from SANS data for **P3HT-*b*-P3HTPMe$_3$(SDS)$_x$** in D_2O: α is the scattering exponent of the defined q region. L_{core}, r_{core} and T_{shell} are the core length, core radius and shell thickness, respectively, obtained from the best fits to the data using the Core-Shell-Cylinder Model in SasView. $X_{sol\text{-}core}$ and $X_{sol\text{-}shell}$ are the calculated solvent fractions in the core and shell, respectively. Unless otherwise stated the data were fit over the entire q-range of 0.08 < q < 2.2 nm^{-1}.

Sample	$q^{-\alpha}$ (q<0.02)	$q^{-\alpha}$ (0.02<q<0.07)	$q^{-\alpha}$ (q>0.07)	Model	L_{core} (nm)	r_{core} (nm)	T_{shell} (nm)	T_{sheet} (nm)	$X_{sol\text{-}core}$	$X_{sol\text{-}shell}$
P3HT-*b*-P3HTPMe$_3$	-1.61 ± 0.15	-5.42 ± 0.08	-2.64 ± 0.72	Core-shell cylinder	51.8	4.7	6.9	-	0.05	0.82
***x* = 0.2**	-1.17 ± 0.05	-5.02 ± 0.08	-2.71 ± 0.35	Core-shell cylinder	58.1	3.4	7.6	-	0.09	0.76
***x* = 0.5**	-1.41 ± 0.06	-4.31 ± 0.10	-3.68 ± 0.32	Core-shell cylinder	54.1	4.9	8.7	-	0.01	0.79
***x* = 1.0**	-1.90 ± 0.04	-3.21 ± 0.16	-3.52 ± 0.30	Lamellar	-	-	-	5.9	0.60	-
***x* = 2.0**	-1.87 ± 0.08	-2.83 ± 0.13	-4.00 ± 0.18	Sheets	-	-	-	8.8	0.83	-
***x* = 5.0**	-1.68 ± 0.10	-1.97 ± 0.14	-4.00 ± 0.10	Sphere [a]	-	2.7	-	-	-	-
***x* = 20.0**	-	-	-4.00 ± 0.34	Sphere [a]	-	2.3	-	-	-	-

[a] These data were only fit between 0.27 and 2.4 nm^{-1} with fitted scattering length densities (SLDs) of 2.38 × 10^{-4} nm^{-2} and 3.63 × 10^{-4} nm^{-2} for x = 5.0 and x = 20.0, respectively. It was not possible to calculate the solvent fraction.

Table S6. Structural parameters obtained from SANS data for **P3HT-*b*-P3HTPMe$_3$**(d_{25}-**SDS**)$_x$ in D_2O: α is the scattering exponent of the defined q region. L_{core}, r_{core} and T_{shell} are the core length, core radius and shell thickness, respectively, obtained from the best fits to the data using the Core-Shell-Cylinder and Lamellar Models in SasView. $X_{sol\text{-}core}$ and $X_{sol\text{-}shell}$ are the calculated solvent fractions in the core and shell, respectively. Unless otherwise stated the data were fit over the entire q-range of $0.08 < q < 2.2$ nm^{-1}.

Sample	$q^{-\alpha}$ (q<0.02)	$q^{-\alpha}$ (0.02<q<0.07)	$q^{-\alpha}$ (q>0.07)	**Model**	L_{core} (nm)	r_{core} (nm)	T_{shell} (nm)	T_{sheet} (nm)	$X_{sol\text{-}core}$	$X_{sol\text{-}shell}$
P3HT-*b*-P3HTPMe$_3$	-1.61 ± 0.15	-5.42 ± 0.08	-2.64 ± 0.72	Core-shell cylinder	51.8	4.7	6.9	-	0.05	0.82
***x* = 0.2**	-1.49 ± 0.06	-5.41 ± 0.06	-2.16 ± 0.27	Core-shell cylinder	48.3	3.9	6.5	-	0.02	0.75
***x* = 0.5**	-1.74 ± 0.03	-4.95 ± 0.09	-1.71 ± 0.13	Core-shell cylinder	47.6	4.0	7.1	-	0.10	0.82
***x* = 1.0**	-1.97 ± 0.07	-4.64 ± 0.08	-3.07 ± 0.21	Core-shell cylinder	47.7	5.0	7.1	-	0.02	0.81
***x* = 2.0**	-1.58 ± 0.02	-4.06 ± 0.11	-1.97 ± 0.27	Lamellar	-	-	-	7.8	-	-
***x* = 5.0**	-1.54 ± 0.08	-4.04 ± 0.08	-3.19 ± 0.48	Lamellar	-	-	-	8.2	-	-
***x* = 20.0**	-1.51 ± 0.03	-3.89 ± 0.16	-1.42 ± 0.49	Lamellar	-	-	-	8.1	-	-

3.5.2 Effect of Hydrogenated *vs*. Perfluorinated Surfactants on the SANS Fitting Parameters of CPE-SDS Complexes.

Table S7. Structural parameters obtained from SANS data for pure **P3HTPMe$_3$** and **P3HTPMe$_3$** with a 1:1 charge ratio of PFOS, d_{25}-SDS and SDS in D_2O. α is the scattering exponent of the defined q region. R_g is the radius of gyration calculated from the corresponding Guinier plot. T_{sheet} is the sheet thickness, respectively, obtained from the best fits to the data using the Lamellar Model in SasView. X_{sol} is the calculated solvent fractions in the sheet. Unless otherwise stated the data were fit over the entire q-range of $0.08 < q < 2.2$ nm^{-1}.

Sample	$q^{-\alpha}$ ($q < 0.02$)	Model	R_g (nm)	T_{sheet} (nm)	X_{sol}
P3HTPMe$_3$	-	-	2.1	-	-
with **PFOS**	-2.31 ± 0.07	Lamellar	-	4.8	0.71
with **d_{25}-SDS**	-2.69 ± 0.02	Lamellar	-	3.4	0.6
with **SDS**	-2.61 ± 0.04	Lamellar	-	2.0	0.37

Table S8. Structural parameters obtained from SANS data for pure **P3HT-*b*-P3HTPMe$_3$** and **P3HT-*b*-P3HTPMe$_3$** with a 1:1 charge ratio of PFOS, d_{25}-SDS and SDS in D_2O. α is the scattering exponent of the defined q region. L_{core}, $r_{core,}$ T_{shell} and T_{sheet} are the core length, core radius, shell thickness and sheet thickness, respectively, obtained from the best fits to the data using the Core-Shell Cylinder and Lamellar Models in SasView. $X_{sol\text{-}core}$ and $X_{sol\text{-}shell}$ are the calculated solvent fractions in the core and shell, respectively. Unless otherwise stated the data were fit over the entire q-range of $0.08 < q < 2.2$ nm^{-1}.

Sample	$q^{-\alpha}$ ($q < 0.02$)	$q^{-\alpha}$ ($0.02 < q < 0.07$)	$q^{-\alpha}$ ($q > 0.07$)	Model	L_{core} (nm)	r_{core} (nm)	T_{shell} (nm)	T_{sheet} (nm)	$X_{sol\text{-}core}$	$X_{sol\text{-}shell}$
CPE	-1.61 ± 0.15	-5.42 ± 0.08	-2.64 ± 0.72	Core-shell cylinder	51.8	4.7	6.9	-	0.05	0.82
with **PFOS**	-2.23 ± 0.01	-4.81 ± 0.12	-2.77 ± 0.45	Core-shell cylinder	46.7	5.9	7.8	-	0.16	0.85
with **d_{25}-SDS**	-1.97 ± 0.04	-4.64 ± 0.08	-3.07 ± 0.21	Core-shell cylinder	47.7	4.9	7.1	-	0.02	0.81
with **SDS**	-1.90 ± 0.04	-3.21 ± 0.16	-3.52 ± 0.30	Lamellar	-	-	-	5.9	0.60	-

3.5.3 Effect of Solvent on the SANS Fitting Parameters of CPE-SDS Complexes.

Table S9. Structural parameters obtained from SANS data for **P3HTPMe$_3$** and **P3HTPMe$_3$(SDS)$_1$** in d_4-MeOD: α is the scattering exponent of the defined q region. L, r and L_{Kuhn} are the length, radius and Kuhn length, respectively, obtained from the best fits to the data using the Cylinder, Flexible Rod and Lamellar Models in SasView. X_{sol} is the calculated solvent fraction in the aggregate. Unless otherwise stated the data were fit over the entire q-range of $0.08 < q < 2.2$ nm^{-1}.

Sample	$q^{-\alpha}$ ($q < 0.02$)	$q^{-\alpha}$ ($0.02 < q < 0.07$)	Model	L (nm)	r (nm)	L_{Kuhn} (nm)	T_{sheet} (nm)	X_{sol}
P3HTPMe$_3$	-1.22 ± 0.02	-1.22 ± 0.02	Cylinder	286.5	1.3	-	-	0.79
			Flexible Cylinder	90.1	1.3	22.6	-	0.85
P3HTPMe$_3$(SDS)$_1$	-1.86 ± 0.04	-2.50 ± 0.04	Lamellar Sheet	-	-	-	4.7	~0.50

Table S10. Structural parameters obtained from SANS data for **P3HT-*b*-P3HTPMe$_3$** and **P3HT-*b*-P3HTPMe$_3$(SDS)$_1$** in d_4-MeOD: SLD_{sol} is the scattering length density of the solvent, α is the scattering exponent of the defined q region. L_{core}, r_{core} and T_{shell} are the core length, core radius and shell thickness, respectively, obtained from the best fits to the data using the Core-Shell Cylinder Model in SasView. $X_{sol\text{-}core}$ and $X_{sol\text{-}shell}$ are the calculated solvent fractions in the core and shell, respectively. Unless otherwise stated the data were fit over the entire q-range of $0.08 < q < 2.2$ nm^{-1}.

Sample	$q^{-\alpha}$ ($q < 0.02$)	$q^{-\alpha}$ ($0.02 < q < 0.07$)	$q^{-\alpha}$ ($q > 0.07$)	L_{core} (nm)	r_{core} (nm)	T_{shell} (nm)	$X_{sol\text{-}core}$	$X_{sol\text{-}shell}$
P3HT-*b*-P3HTPMe$_3$	-1.81 ± 0.10	-4.39 ± 0.05	-1.90 ± 0.13	57.3	5.3	7.7	0.15	0.86
P3HT-*b*-P3HTPMe$_3$(SDS)$_1$	-1.82 ± 0.07	-4.93 ± 0.04	-1.64 ± 0.14	54.3	5.4	7.4	0.19	0.85

7. Supporting Cryo-TEM Figures

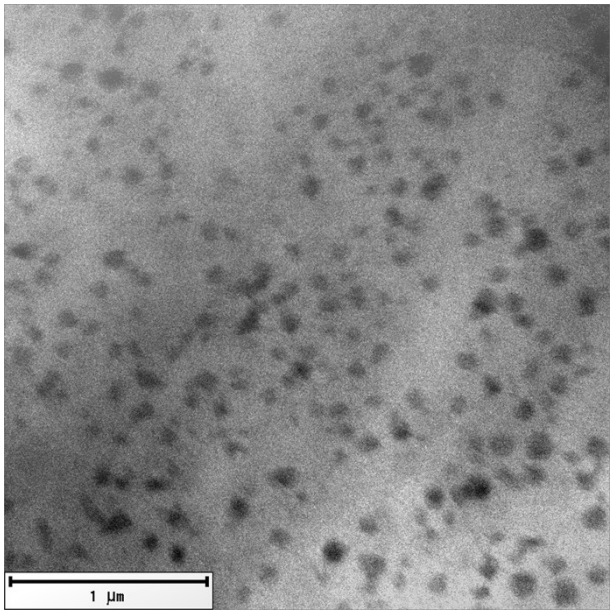

Figure S8. Cryo-TEM micrograph of **P3HTPMe$_3$(SDS)**. Total concentration = 10 mg mL^{-1}.

8. AFM Images of CPE and Surfactant Thin Films

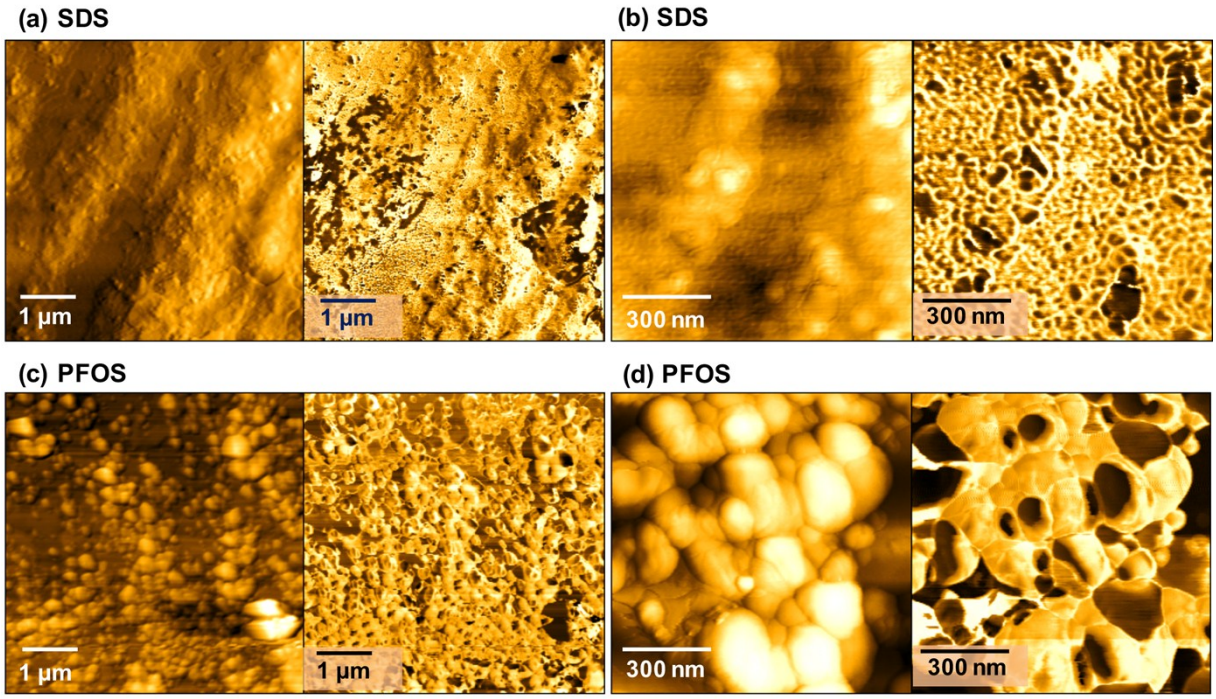

Figure S9. AFM tapping mode images of (a,b) **SDS** and (c,d) **PFOS.** Drop-cast onto silicon from solutions of surfactants in D_2O (10 mg mL^{-1}). Left: height images; right: phase images.

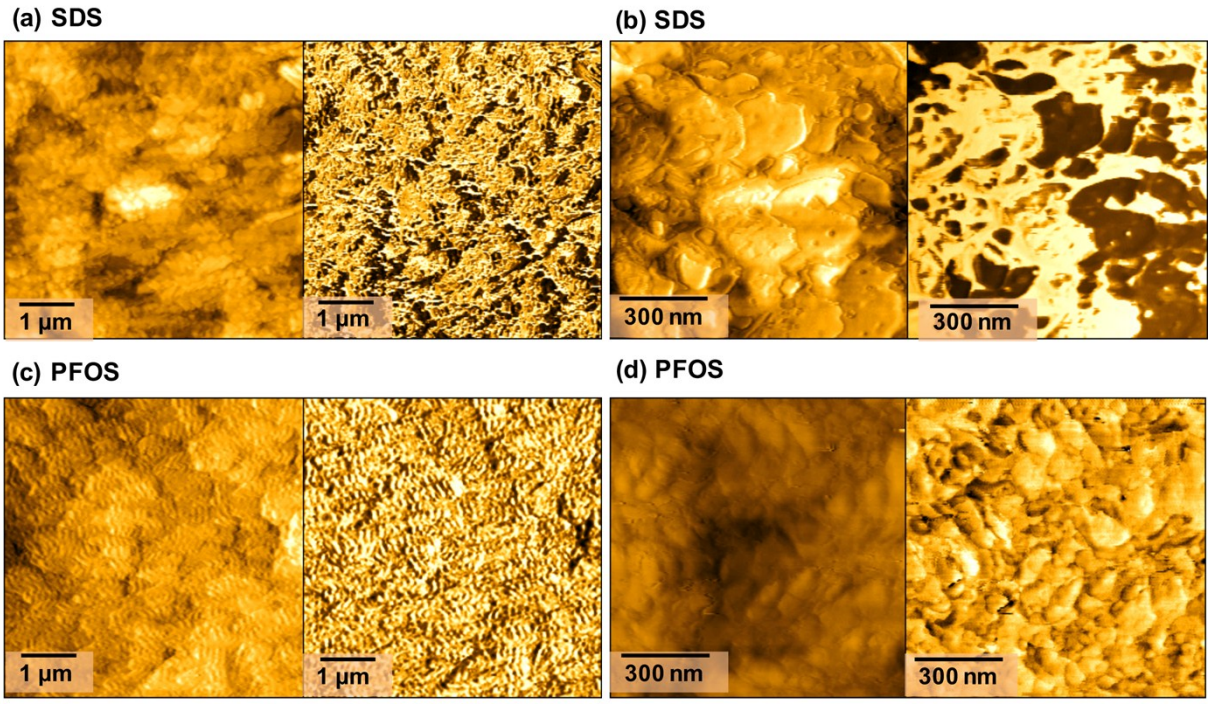

Figure S10. AFM tapping mode images of (a,b) **SDS** and (c,d) **PFOS.** Spin-coated onto silicon from solutions of surfactants in MeOH (10 mg mL^{-1}). Left: height images; right: phase images.

7. References

1. http://www.sasview.org/index.html
2. A. Guinier and G. Fournet, *Small Angle Scattering of X-rays*, John Wiley and Sons, 1955.
3. A. A. Golosova, J. Adelsberger, A. Sepe, M. A. Niedermeier, P. Lindner, S. S. Funari, R. Jordan and C. M. Papadakis, *J. Phys. Chem. C*, 2012, **116**, 15765-15774.
4. I. Livsey, *J. Chem. Soc. Faraday Trans.*, 1987, **83**, 1445-1452.
5. J. Berghausen, J. Zipfel, P. Lindner and W. Richtering, *J. Phys. Chem. B*, 2001, **105**, 11081-11088.
6. F. Nallet, R. Laversanne and D. Roux, *J. Phys. II France*, 1993, **3**, 487-502.